

Implementation of local and high-fidelity quantum conditional phase gates in a scalable two-dimensional ion trap

Ping Zou, Jian Xu, Wei Song, and Shi-Liang Zhu*
*Laboratory of Quantum Information Technology, ICMP and SPTE,
South China Normal University, Guangzhou 510006, China*

We propose a scheme to implement high-fidelity conditional phase gates on pair of trapped ions immersed in a two-dimensional Coulomb crystal, using interaction mediated by all axial modes without side-band addressing. We show through numerical calculations that only local modes can be excited to achieve entangling gates through shaping the laser beams, so that the complexity of the quantum gate does not increase with the size of the system. These results suggest a promising approach for realization of large scale fault-tolerant quantum computation in two dimensional traps architecture.

PACS numbers: 03.67.Pp, 03.65.Vf, 03.67.Lx, 32.80.Qk

Keywords: Quantum computation, Ion trap, Scalability, Conditional phase gate

I. INTRODUCTION

The trapped ion system is one of the most promising candidates for quantum computation[1]. In the system, each qubit is formed by the long lived internal atomic levels of each ion, and laser beams have been used to manipulate quantum states of ions[2, 3]. Different theoretical schemes have been proposed for quantum gate operations with the aid of the ion's collective motions[2, 3, 4, 5, 6, 7] and many have been experimentally demonstrated with small numbers of qubits [8, 10, 11, 12].

To make a quantum computer have practical value, scalability of proposed architectures to many qubits is of central importance. However, scaling up to tens of qubits in ion-trapped system proves to be a great challenge and many efforts have been done in this area. The main difficulty of the scalability is that the sideband addressing, which is believed to be necessary in the gate operations proposed in most schemes, becomes impossible as the ion number increase. There are two promising approaches in literature to overcome this scalar difficulty. One is to divide the trapped-ion quantum computer into operation region and memory region. Quantum gate operations are always implemented at the operation region where only a few ions form a small linear ion chains, while ions can be shuttled between the operation and memory regions [13]. The other promising approach is to use appropriately shaped laser pulses to realize high-fidelity conditional quantum gates, where all phonon modes are considered in the gate operations even in a very large linear ion crystal[14]. This approach may be significantly strengthened in an improved scheme [15] where the tightly confined transverse modes[7] are used to mediate quantum gate operations and an anharmonic trap potential is proposed to arrange the ions in a uniformly-spaced linear crystal. In this approach, the gate operation has a local character so that the complexity of the operations does

not depend on the chain size[6].

To date most studies are limited to system of the linear trap with ions laser-cooled and confined in one dimensional crystals, little attention has been payed to the two-dimensional crystals[16, 17, 18]. Today penning trap can confine a large number of ions ($10^4 - 10^6$) by a potential with approximate cylindrical symmetry [19, 20]. In penning trap, axial confinement is realized by a static electric field, while radial trap potential is induced by the rotations of the ions under an axial magnetic field. Under certain parameters the ions will be arrayed in a two-dimensional plane with separation of order of tens of microns, such that they are individually addressable by optical means. Although the rotation of the ion crystal may induce additional technical difficulty in the addressing of the ions, quantum manipulation of such qubits is still possible. Particularly it has been proposed that the axial phonon modes, which are independent on the phonon modes in the planar direction since the anharmonic effects of phonon modes are negligible, can be used in the conditional gate operations[16]. However, the phonon modes in a two-dimensional crystal are much more complicated than that of a linear ion crystal, and such complex mode spectrum makes it more difficult to resolve individual modes for quantum gate operations. Clearly the two-dimensional penning trap may provide an almost ideal system for scalable quantum computation and quantum simulation if the aforementioned difficulty of sideband addressing can be overcome. Therefore, a practical scheme to achieve the conditional gate operations without sideband addressing, which has not been touched before in such large scale two-dimensional traps, is highly needed.

In this paper, we propose a feasible scheme to implement high-fidelity conditional phase gates without sideband addressing in the scalable two-dimensional traps. We investigate in detail the configurations of the ions as well as the normal modes of the two-dimensional crystals. This scheme uses the ion's motion along the axial direction. Although the effects of phonon modes in the planar direction can be neglected, the axial phonon mode spec-

*Electronic address: shilzhu@yahoo.com.cn

trum is still too complicated to be resolved in the gate operations. We show that the local modes suggested in Ref.[6, 14, 15] can also be applied to mediate the interaction between ion and laser beams, so that the complexity of the quantum gate does not increase with the size of the system. Compared to the scheme proposed in Ref[16], we can implement conditional gate faster by optimally controlling the pulse shape. Since the nearest-neighbor entangling quantum gates are sufficient for fault-tolerant quantum computing in two dimensional trap, in sharp contrast to one dimensional chain where the nearest-neighbor entangling quantum gates are insufficient[23], the generalization to two dimensional trap proposed here will be very useful.

The paper is organized as follows: In Sec. II we study the equilibrium positions of the ions trapped in the two dimensional penning trap. In Sec. III we present the normal modes of the trapped ions and especially investigate the properties of the axial modes in detail. In Sec. IV we show how to implement the conditional phase gates with high fidelity using the axial modes. A summary of our results and a conclusion are presented in Sec. V.

II. EQUILIBRIUM POSITIONS OF IONS IN A TWO-DIMENSIONAL HARMONIC TRAP

The system we have in mind is a two-dimensional trap [19, 20, 21] with N ions confined in a harmonic external potential. Including their mutual Coulomb repulsion interaction the potential energy of ions is given by

$$V = \frac{1}{2}M \sum_{n=1}^N (\omega_x^2 x_n^2 + \omega_y^2 y_n^2 + \omega_z^2 z_n^2) + \sum_{n<l}^N \frac{e^2}{4\pi\epsilon_0} \frac{1}{r_{nl}}, \quad (1)$$

where $\mathbf{r}_n \equiv (x_n, y_n, z_n)$ denotes the position of the n th ion, M is the mass of each ion, e is the electron charge, ϵ_0 is the permittivity of free space and $r_{nl} = \sqrt{(x_n - x_l)^2 + (y_n - y_l)^2 + (z_n - z_l)^2}$ is the distance between the n -th and l -th ions. Here ω_η ($\eta = x, y, z$) is the trap frequency which characterizes the strength of the trapping potential in the η direction. In the paper we assume that $\omega_x = \omega_y = \omega_r$ and $\beta = \omega_z/\omega_r$. The parameter β is a measure of the trap anisotropy and it will uniquely determine the ionic crystal structure for given N [22].

Similarly to what they do in Ref[24] for the 1D linear case, to determine the equilibrium positions of ions, we may expand the position of the n th ion around its equilibrium position $\mathbf{r}_n^{(0)}$ as $\mathbf{r}_n(t) \approx \mathbf{r}_n^{(0)} + \mathbf{q}_n(t)$, where $\mathbf{q}_n(t)$ is a small displacement. The equilibrium positions are determined by the conditions

$$\left[\frac{\partial V}{\partial \mathbf{r}_n} \right]_{\mathbf{r}_n = \mathbf{r}_n^{(0)}} = 0,$$

and its dimensionless form $\mathbf{u}_m = \mathbf{r}_m^{(0)}/\ell$ ($m = 1, 2, \dots, N$) with $\ell = \sqrt[3]{e^2/4\pi\epsilon_0 M \omega_r^2}$ can be described by a set of $3N$

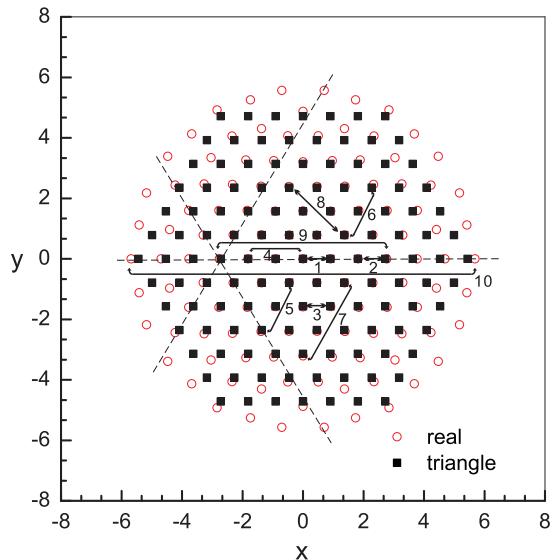


FIG. 1: (Color online). The Configuration of ion crystals for the number of ions $N = 127$. The circles represent the equilibrium positions of ions obtained by numerical calculation. For comparison, the solid squares denote the configuration of an ideal triangular lattice. Conditional phase gates acting on 10 pairs of ions connected by arrows are studied.

equations given as

$$u_m^x - \sum_{n=1, n \neq m}^N \frac{(u_n^x - u_m^x)}{\ell_{nm}^3} = 0, \quad (2)$$

$$u_m^y - \sum_{n=1, n \neq m}^N \frac{(u_n^y - u_m^y)}{\ell_{nm}^3} = 0, \quad (3)$$

$$u_m^z - \frac{1}{\beta^2} \sum_{n=1, n \neq m}^N \frac{(u_n^z - u_m^z)}{\ell_{nm}^3} = 0, \quad (4)$$

where $\ell_{nm} = \sqrt{(u_n^x - u_m^x)^2 + (u_n^y - u_m^y)^2 + (u_n^z - u_m^z)^2}$ denotes the dimensionless distance between ions n and m .

Determined by the number of ions and the trapped frequencies $\omega_{x,y,z}$, the ions may form a string, a 2D or 3D ionic crystals[22]. To individually address qubits by laser beams, we usually assume ions are confined in a 1D or 2D crystals. The 1D case has been extensively studied, but less work focussing on the 2D traps[16, 18]. In this paper we pay attention to the latter. Assume that ω_z is strong enough such that the configuration of ions in a 2D plane is always stable (the detailed requirement will be addressed below), then the equilibrium positions are confined in $x-y$ plane and $u_m^z = 0$ for an arbitrary ion. Under this condition, the equilibrium positions in $x-y$ plane may be determined by solving Eq.(2) and Eq.(3). The solutions are not unique, for instance, ions for $N = 4$ may locate at

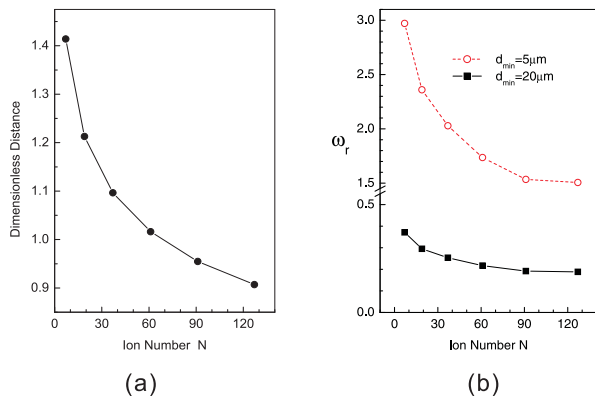


FIG. 2: (a) Dimensionless minimum separation as a function of total number of ions N in a 2D harmonic trap. (b) The trap frequency $\omega_r/2\pi$ (MHz) required for the minimum of distance $d_{min} = 5\mu m$, $20\mu m$ as a function of N . Only the data for $N = 7, 19, 37, 61, 91, 127$ are given.

the vertexes of a triangle and its center point or locate at the vertexes of a square. However, both experiments and theories show that the stable configuration of large number of ions forms a distortional hexagonal lattice[19, 22], while the inner region arranges in equilateral triangles. In Ref.[19] laser-cooled ${}^9\text{Be}^+$ ions in a two-dimensionally extended lattice planes were directly observed, especially a single plane hexagonal structure was observed, which is the configuration we want to utilize. For concreteness, in this paper we study the case where finite ions form the symmetric triangular lattice, such as the ion numbers are $N = 7, 19, 37, 61, 91, 127, \dots$. The configuration for $N = 127$ is shown in Fig. 1. In an ideal triangular lattice, the equilibrium position $\mathbf{r}^{(0)}$ may be expressed as $\mathbf{r}^{(0)} = [(j + l/2)a_0, \sqrt{3}a_0/2]$ with a_0 denoting the lattice constant, j and l being integers. As expected the equilibrium positions of ions obtained by numerical calculation exhibit little deflection from the ideal configuration. As seen from Fig. 1, the lattice spacings are not constant. As the ions get farther from the center, the lattice spacings become larger; however, it is almost constant near the crystal center and we get a nice triangular lattice at the center that can be suitable for the implementation of quantum computation.

To manipulate quantum states of ions by laser beams, addressing individually the ions by optical means are needed, thus the minimum interior spacing must be larger than the size of the focal spot of the laser beam which is about $4\mu m$ in the experiments. The distances between the ions depend on the strength of the confining potentials as well as the number of ions. Actually the minimum value d_{min} of the dimensionless distance between two adjacent ions descends as the total number of the ions is increased. By numerical fit from $N = 7$ to 217, we find it obeys the relation $u_{min} \approx 1.995/N^{0.172}$, which is a slower rate than $2.018/N^{0.559}$ [24] in the linear chain case. The typical scaled distances u_{min} in 2D trap with small ion number N are shown in Fig. 2a. The relation

between inter particle spacing $d_{min} = u_{min}\ell$ and the frequency ω_r is $\omega_r = \sqrt{\frac{e^2 u_{min}^3}{4\pi\epsilon_0 M d_{min}^3}}$, so ω_r has an upper limit. The examples with small N are shown in Fig. 2b.

III. NORMAL MODES

We now turn to investigate the normal modes that are useful in the construction of the quantum operations in ion-trapped quantum computation. The normal modes in a linear trap has been studied in detail in Ref.[24], here we generalized the approach in one-dimensional crystal to two-dimensional penning trap. In a realistic ion trap the ions will have some nonzero temperature and will move around their equilibrium positions. However, if the ions are sufficiently cold, we may expand the potential V under the harmonic approximation (i.e., the terms $O(\mathbf{q}^3)$ can be neglected), and obtain $V = 1/2 \sum_{n,m} \mathbf{q}_n \mathbf{q}_m [\partial^2 V / \partial \mathbf{r}_n \partial \mathbf{r}_m]_0$. Here the subscript 0 denotes that the double partial derivative is evaluated at $\mathbf{q}_n = \mathbf{q}_m = 0$. In this case, the Lagrangian for the small oscillations is given by

$$L = \frac{M}{2} \sum_{n=1}^N (\dot{\mathbf{q}}_n)^2 - \frac{1}{2} \sum_{n,m=1}^N \mathbf{q}_n \mathbf{q}_m \left[\frac{\partial^2 V}{\partial \mathbf{r}_n \partial \mathbf{r}_m} \right]_0. \quad (5)$$

The anharmonic terms in V will induce small errors and can be neglected, which has been proved in Ref. [16]. The double partial derivatives in Eq.(5) may be calculated explicitly, then the Lagrangian for the resulting small oscillations is found as

$$L = \frac{M}{2} \sum_{n=1}^N (\dot{\mathbf{q}}_n)^2 - \frac{M\omega_r^2}{2} \sum_{n,m=1}^N A_{nm}^{zz} q_n^z q_m^z - \frac{M\omega_r^2}{2} \sum_{n,m=1}^N (A_{nm}^{xx} q_n^x q_m^x + 2A_{nm}^{xy} q_n^x q_m^y + A_{nm}^{yy} q_n^y q_m^y),$$

where

$$A_{nm}^{xx} = \begin{cases} 1 + \sum_{p=1, p \neq m}^N \frac{2(u_m^x - u_p^x)^2 - (u_m^y - u_p^y)^2}{[(u_m^x - u_p^x)^2 + (u_m^y - u_p^y)^2]^{5/2}}, & (n = m) \\ \frac{-2(u_m^x - u_p^x)^2 + (u_m^y - u_p^y)^2}{[(u_m^x - u_p^x)^2 + (u_m^y - u_p^y)^2]^{5/2}}, & (n \neq m) \end{cases} \quad (6)$$

$$A_{nm}^{xy} = \begin{cases} \sum_{p=1, p \neq m}^N \frac{3(u_m^x - u_p^x)(u_m^y - u_p^y)}{[(u_m^x - u_p^x)^2 + (u_m^y - u_p^y)^2]^{5/2}}, & (n = m) \\ \frac{-3(u_m^x - u_p^x)(u_m^y - u_p^y)}{[(u_m^x - u_p^x)^2 + (u_m^y - u_p^y)^2]^{5/2}}, & (n \neq m) \end{cases} \quad (7)$$

$$A_{nm}^{yy} = \begin{cases} 1 + \sum_{p=1, p \neq m}^N \frac{-(u_m^x - u_p^x)^2 + 2(u_m^y - u_p^y)^2}{[(u_m^x - u_p^x)^2 + (u_m^y - u_p^y)^2]^{5/2}}, & (n = m) \\ \frac{(u_m^x - u_p^x)^2 - 2(u_m^y - u_p^y)^2}{[(u_m^x - u_p^x)^2 + (u_m^y - u_p^y)^2]^{5/2}}, & (n \neq m) \end{cases} \quad (8)$$

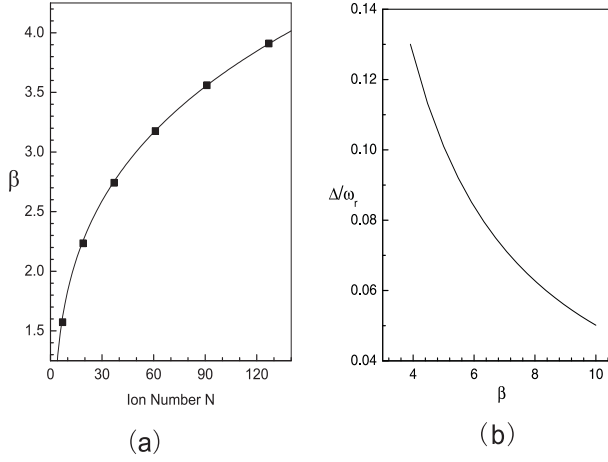


FIG. 3: (a) The minimum β required to confine all ions in a 2D plane as a function of total number of ions in the Penning trap. Only the data for $N = 7, 19, 37, 61, 91, 127$ are given. The line represents the best-fit behavior of the trend. (b) The energy gap of the axial modes between the center of mass mode and its nearest mode as a function of β .

$$A_{nm}^{zz} = \begin{cases} \beta^2 - \sum_{p=1, p \neq m}^N \frac{1}{[(u_m^x - u_p^x)^2 + (u_m^y - u_p^y)^2]^{3/2}}, & (n = m) \\ \frac{1}{[(u_m^x - u_p^x)^2 + (u_m^y - u_p^y)^2]^{3/2}}. & (n \neq m) \end{cases} \quad (9)$$

In term of the normal phonon modes, the motional Hamiltonian H_0 for $3N$ motional modes can be written as the standard form

$$H_0 = \sum_{k=1}^{3N} \hbar\omega_k (a_k^\dagger a_k + \frac{1}{2}),$$

which includes three possible polarization: axial (\mathbf{z}) modes and two in-plane (\mathbf{x}, \mathbf{y}) modes with the eigenfrequency ω_k . The axial and in-plane modes are independent, and the axial modes are determined by the matrix A^{zz} . The eigen-frequencies $\omega_{z,k} \equiv \sqrt{\mu_{z,k}}\omega_r$ and eigenvectors $\mathbf{b}_j^{z,k}$ of the axial modes are obtained from diagonalization of the matrix A^{zz} with $\sum_n A_{nj}^{zz} \mathbf{b}_n^{z,k} = \mu_{z,k} \mathbf{b}_j^{z,k}$. To make ions stable in the plane, all the angular frequency of the axial phonon modes $\omega_{z,k}$, then the eigenvalues $\mu_{z,k}$ of the matrix $A^{zz}(\beta)$ must be positive. Therefore, the equation $\mu_{z,k} = 0$ can be considered as the critical equation to determine the stability of the two-dimensional configuration. After solving this equation by numerical calculation, the critical values of β for different ionic number are shown in Fig. 3a. The trend can be well described by a simple power law $\beta = \sqrt{1.073(N-2)^{0.55}}$, approximately coinciding with the results that others obtained when researching the structural transition of the crystalline confined system, such as the empirical scaling laws of Ref.[25], and the theoretic estimation of Ref.[22]. So the critical value of β is the phase transition point

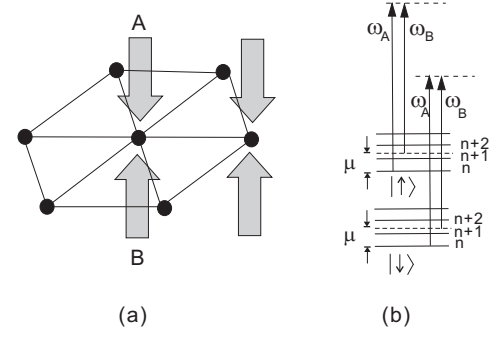


FIG. 4: (a) Quantum gate in a penning trap: electromagnetic fields induce a state-dependent dipole force on two ions in a triangular lattice. (b) A σ_z -dependent force is driven by electromagnetic fields with two frequencies separated by μ . These fields couple the qubit states to the excited states with different coupling strengths, producing a differential AC Stark shift that oscillates at μ . The two fields must have a non-zero wavevector difference along the axial direction[26].

that the 3D ionic structures become oblate to the $x-y$ plane, forming a distorted 2D hexagonal lattice. In the following we assume that the parameter β is larger than the critical values.

The spectrum of the axial modes exhibits some typical features: the center of mass mode at ω_z is the highest frequency axial mode, while the frequency splitting between the center of mass mode and the second-to highest mode is the maximum, and the splitting will become smaller when increasing β , as shown in Fig. 3b. We will impose the axial modes to implement quantum conditional phase gate in the next section.

IV. CONDITIONAL PHASE FLIP GATES

We now start to address quantum gate operations in this two dimensional trap, mediated by many axial phonon modes. To perform quantum gates, we use the ac-Stark shift from two propagating laser beams with a relative angle and detuning to apply spin-dependent force on the ions along the z direction (see FIG.4) as they did in experiments [8, 10, 26]. Under the Lamb-Dicke condition the Hamiltonian of the system in the rotating-wave approximation becomes[5, 14]

$$H = - \sum_{n,k=1}^N F_n(t) g_n^k (a_k^\dagger e^{i\omega_{z,k}t} + a_k e^{-i\omega_{z,k}t}) \sigma_n^z, \quad (10)$$

where $\sigma_n^z = |0\rangle\langle 0| - |1\rangle\langle 1|$ is the Pauli operator, $F_n(t)$ is the spin-dependent force acting on the n th ion, and $g_n^k = \sqrt{\hbar/2M\omega_{z,k}} \mathbf{b}_n^{z,k}$ is the coupling constant between the n th ion and the k th phonon mode, $\mathbf{b}_n^{z,k}$ are the eigenvectors of the matrix A^{zz} defined in the previous section. The spin-dependent force has the form of $\Omega \sin(\mu t)$ deriving from the ac Stark shift from the Raman laser beams, where μ is the detuning between the Raman laser beams

pair number	$\omega_r/2\pi = 0.2$			$\omega_r/2\pi = 1.0$		
	F	μ	Ω^M	F	μ	Ω^M
1	0.999	10.033	0.177	0.994	10.076	0.443
2	0.999	10.033	0.178	0.989	10.076	0.442
3	0.999	10.033	0.173	0.990	10.045	0.356
4	0.998	10.033	0.363	0.989	10.045	0.443
5	0.998	10.033	0.169	0.985	10.076	0.577
6	0.998	10.033	0.369	0.973	10.025	0.534
7	0.997	10.033	0.566	0.978	10.025	0.489
8	0.997	10.033	0.492	0.979	10.025	0.505
9	0.997	10.087	2.768	0.940	10.076	1.090
10	0.995	10.040	4.040	0.690	10.076	1.315

TABLE I: The gate fidelity F for 10 pairs of ions labeled in Fig.1 with the same ω_z (10MHz) but two different ω_r . The units for the detuning μ and the maximum Rabi frequency Ω^M are 1.0MHz.

and Ω is the two photon Rabi frequency. The evolution operator determined by Hamiltonian (10) can be explicitly found as[27]

$$U(\tau) = e^{i\sum_n \phi_n(\tau)\sigma_n^z + i\sum_{l < n} \phi_{ln}(\tau)\sigma_l^z \sigma_n^z}, \quad (11)$$

where $\phi_n(\tau) = \sum_k [\alpha_n^k(\tau)a_k^\dagger - \alpha_n^{k*}(\tau)a_k]$ with $\alpha_n^k(\tau) = \frac{i}{\hbar} \int_0^\tau F_n(t)g_n^k e^{i\omega_{z,k}t} dt$ representing the residual entanglement between ion n and phonon mode k , and $\phi_{ln}(\tau) = \frac{2}{\hbar^2} \int_0^\tau dt_2 \int_0^{t_2} \sum_k F_l(t_2)g_l^k g_n^k F_n(t_1) \sin \omega_{z,k}(t_2 - t_1) dt_1$ characterizes the effective qubit-qubit interaction between ions l and n . Note that the phase $\phi_{ln}(\tau)$ is actually a kind of unconventional geometric phase factor[27, 28], which has been experimentally demonstrated to have advantage of high-fidelity[8, 9].

Eq.(11) is actually a conditional phase flip (CPF) gate acting on ions n and l if $\phi_n(\tau) = \phi_l(\tau) = 0$ and $\phi_{nl}(\tau) = \pi/4$. To implement a CPF gate on arbitrary ions n and l , we make the spin dependent force to be nonzero only for these two ions with $F_n(t) = F_l(t) = F(t)$, and set the gate time τ so that $\phi_n(\tau) = \phi_l(\tau) = 0$ and $\phi_{nl}(\tau) = \pi/4$. In principle, it is always possible to satisfy these constraints by designing a sufficiently complicated pulse shape for the force.

Taking the method in Ref. [14], we use a simple sequence of laser pulses which take minimum experimental control. A continuous-wave laser beam is chopped into m equal-time segments, with a constant but controllable Rabi frequency Ω_p for the p th ($p = 1, 2, \dots, m$) segment. The spin dependent force $F(t)$ then takes the form $F(t) = \Omega_p \sin(\mu t)$ for the time interval $(p-1)\tau/m \leq t < p\tau/m$. With a small number of control parameters Ω_p , $\alpha_n^k(\tau)$ (then $\phi_i(\tau)$) in the evolution operation may not be exact zero, but as long as they are small enough, we still can get a high-fidelity gate. The task is to find an optimal control laser beam parameters sequence Ω_p and μ to get a small enough infidelity $F_{in} (\equiv 1 - F$ with F being the gate fidelity). The gate fidelity is defined as $F = \langle \Psi_f | \rho_r | \Psi_f \rangle$, where $|\Psi_f\rangle$ is the ideal output state after implement the CPF gate on the initial state $|\Psi_0\rangle$ which chosen typically as $|\Psi_0\rangle = (|0\rangle_i + |1\rangle_i) \otimes (|0\rangle_j + |1\rangle_j)/2$, and the

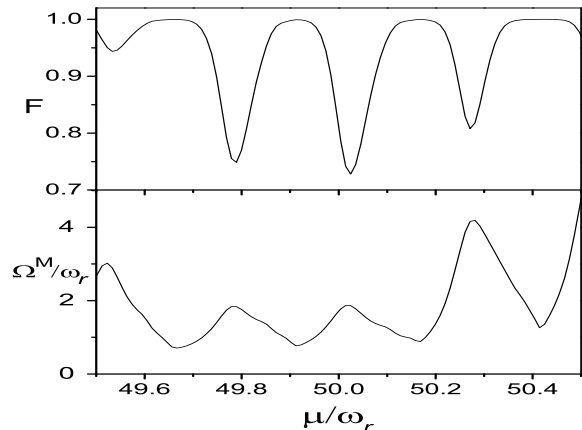


FIG. 5: The gate fidelity F and the maximum Rabi frequency Ω^M as a function of the laser detuning μ for ions pair 1 with $\omega_r/2\pi = 0.2$ MHz, $\omega_z/2\pi = 10.0$ MHz and gate time $50\mu s$.

density operator $\rho_r = Tr_m(U(\tau)(|\Psi_0\rangle\langle\Psi_0| \otimes \rho^B)U(\tau)^\dagger)$ with tracing over the motional states of all the ions. Here we have assume that the phonon modes are initially in thermal state ρ^B with an effective temperature T .

Interestingly, we find that a very simple sequence of laser pulses (such as $m = 5$) can ensure a good gate fidelity even for the two-dimensional trap. For concreteness, we calculate numerically the CPF gates between 10 pairs of ions labeled in Fig. 1, with the same gate time $\tau = 50\mu s$ and $\omega_z/2\pi = 10.0$ MHz but two different ω_r . The results are shown in Table I. In Table I, we list the optimal fidelity F , the corresponding detuning μ and the maximum Rabi frequency Ω^M for each gate, where $\Omega^M = \text{Max}\{\Omega_p\}$ can be used to characterize the maximum laser power required in the gate operations. In the numerical calculation, we first calculate the fidelity and the required Rabi frequency for a CPF gate as a function of the detuning. As an example, the results for ion pair 1 with $\omega_r = 0.2$ MHz is shown in Fig. 5, and for any other gate operations the relation between the fidelity and the detuning is similar, so fidelity has a local maximum near the detuning $\mu = \omega_z$. The data in Table I are derived from this approach.

In Table I, the dimensionless distance between the pairs of ions is increasing in sequence. We observe several main features: (i) For both values of ω_r , it is clear that the gate fidelities decrease with the increasing of the distance between the pair of ions. Especially for $\omega_r = 1.0$ MHz, the fidelity decreases relatively quickly with the distance between ions, for example, the fidelity is about 0.994 for the 1st pair of ions, while it becomes 0.690 for the 10th pair of ions. In addition, the laser powers required for the CPF gates generally increase with the distance between the pair of ions. (ii) To understand the influence of minimum ionic separation to the gate fidelity, all gates are performed with two different trap frequency ω_r . One frequency is set as $\omega_r/2\pi = 0.2$ MHz, and the other $\omega_r/2\pi = 1.0$ MHz, then the corresponding

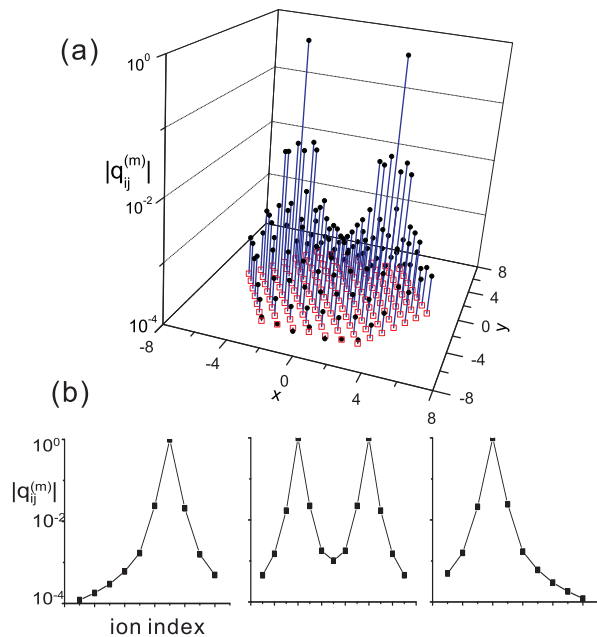


FIG. 6: (Color online). The relative response of the ions for the gate operation. (a) The points (blank squares) in the $x-y$ plane represent the ions in the equilibrium positions and the z values (filled circles) are the maximal deviation $q_{ij}^{(m)}$ from the equilibrium position of the ions during the gate operation. (b) The response of the ions located along the three lines drawn in Fig. 1. The $|q_{ij}^{(m)}|$ for the target ions have been normalized to 1. The fast decay of the response as one moves away from the target ions shows that the gate operation involves vibration of only local ions.

minimum separation are $19.15\mu\text{m}$ and $6.57\mu\text{m}$, respectively. From the table we can see that under condition of the same gate time and ω_z , gate realized in the trap with larger minimum interior spacing will gain a higher fidelity. The physics behind it will be addressed later. On the other hand, it is worth pointing out that, for pairs with larger distance, higher fidelity can be gained with lower ω_r or longer gate time, for example, taking gate time $\tau = 200\mu\text{s}$, the fidelity for the ion pair 10 with $\omega_r/2\pi = 1.0\text{MHz}$ will be above 0.995.

The physics behind such high-fidelity is that the gate has a local character[15], i.e., the contribution to the CPF gate comes primarily from the spin-dependent oscillations of the ions that are close to the target ions. To demonstrate the local properties of the quantum gates, we plot in Fig. 6 the response of each ion during the gate operation between the 9th ion pair with $\omega_r/2\pi = 0.2\text{MHz}$. The figure explicitly exhibits the ultra fast decay of the ions response from the target ions. So the noises from the ionic vibration come just from the nearby ions. We have shown in Table I that the fidelity would be higher for a smaller ω_r , since the ion spacings are less in the larger ω_r . We have calculated the response of all ions for different ω_r , and find that q_{ij}^m of the nearby of the target ions for $\omega_r = 1.0\text{MHz}$ is larger of about

10% than that of $\omega_r = 0.2\text{MHz}$. So one can understand that the fidelity would be lower by the increasing of the frequency ω_r . Attributing to this local character of the gate operations, two notable advantages appear for the quantum computation: (i) the complexity of a gate operation in the two-dimensional traps does not depend on the system size, in sharp contrast to the schemes based on side-band addressing. (ii) The gates on the ions in different regions in the two-dimensional traps can be performed in parallel.

The generalization of local gate operations from the linear trap[7, 15] to two dimensional trap may have advantages in the fault-tolerant quantum computation. It is well known that the set of quantum gates with local entangling quantum gates and single-bit gates are universal for quantum computation. Furthermore, it would be useful for large-scale fault-tolerant quantum computing if the entangling quantum gates can be realized for any pair of qubits. However, although the quantum gates for any pair of ions in a large scale two dimensional trap are possible, they are slow and costly in the sense that the laser powers should be larger and the control parameters should be increased if the distance between ions are large. In this case, an important question is whether it is still possible to perform large-scale fault-tolerant quantum computing with quantum gates that perform only on the ions with the distance much smaller than the size of the trap. The recent studies[23] have shown that in a two-dimensional lattice, even with only nearest-neighbor quantum gates, the error threshold can be still close to a percent level, which is basically as good as the case with arbitrary nonlocal gates, while the nearest-neighbor quantum gates are not sufficient for fault-tolerant quantum computing in one dimensional chain. So the generalization of trapped ion quantum computation to two dimensional trap is highly deserved.

V. CONCLUSIONS

In summary, We have explicitly exhibited the configuration of the two dimensional trap and the equilibrium positions of the ions trapped in small ion number by numerical simulation, and then examined the condition on which all ions are confined in a plane. After investigating the properties of the axial modes of the trapped ions, we have shown through explicit examples and calculations that it is feasible to perform high fidelity CPF gate in the penning traps using the axial modes, and the gate has a local character as in the linear chain case. The results suggest a realistic prospect for realization of large scale quantum computation in the penning traps architecture.

We thank L. M. Duan, G. D. Lin, and M. Yang for helpful discussions. The work was supported by NSF of China under Grant No. 10674049 and the State Key Program for Basic Research of China (Nos.2006CB921801 and 2007CB925204).

-
- [1] For recent review of trapped ion quantum computation, see R. Blatt and D. Wineland, *Nature (London)* **453**, 1008 (2008); H. Häffner, C.F. Roos, and R. Blatt, *Phys. Rep.* **469**, 155-203 (2008).
- [2] J. I. Cirac and P. Zoller, *Phys. Rev. Lett.* **74**, 4091 (1995).
- [3] D. Wineland, C. Monroe, W.M. Itano, D. Leibfried, B. King, and D.M. Meekhof, *J. Res. Natl. Inst. Stand. Technol.* **103**, 259 (1998).
- [4] A. Sorensen and K. Molmer, *Phys. Rev. Lett.* **82**, 1971 (1999); *Phys. Rev. A* **62**, 022311 (2000).
- [5] J. J. Garcia-Ripoll, P. Zoller, and J. I. Cirac, *Phys. Rev. Lett.* **91**, 157901 (2003); *Phys. Rev. A* **71**, 062309 (2005).
- [6] L.-M. Duan, *Phys. Rev. Lett.* **93**, 100502 (2004).
- [7] S. L. Zhu, C. Monroe, and L. -M. Duan *Phys. Rev. Lett.* **97**, 050505 (2006).
- [8] D. Leibfried, B. DeMarco, V. Meyer, D. Lucas, M. Barrett, J. Britton, W. M. Itano, B. Jelenkovic, C. Langer, T. Rosenband, and D. J. Wineland, *Nature (London)* **422**, 412 (2003).
- [9] J. Du, P. Zou, and Z. D. Wang, *Phys. Rev. A* **74**, 020302 (2006).
- [10] P. C. Haljan, K.-A. Brickman, L. Deslauriers, P. J. Lee, and C. Monroe, *Phys. Rev. Lett.* **94**, 153602 (2005).
- [11] H. Häffner, W. Hänsel, C. F. Roos, J. Benhelm, D. Chek-al-kar, M. Chwalla, T. Körberl, U. D. Rapol, M. Riebe, P. O. Schmidt, C. Becher, O. Gühne, W. Dür, and R. Blatt, *Nature (London)* **438**, 643 (2005).
- [12] D. Leibfried, E. Knill, S. Seidelin, J. Britton, R. B. Blakestad, J. Chiaverini, D. B. Hume, W. M. Itano, J. D. Jost, C. Langer, R. Ozeri, R. Reichle, and D. J. Wineland, *Nature (London)* **438**, 639 (2005).
- [13] D. Kielpinsky, C. Monroe, and D. Wineland, *Nature (London)* **417**, 709 (2002).
- [14] S. -L. Zhu, C. Monroe, and L.-M. Duan, *Europhys. Lett* **73**, 485 (2006).
- [15] G. D. Lin, S. L. Zhu, R. Islam, K. Kim, M. S. Chang, S. Korenblit, C. Monre, and L. M. Duan, *Europhys. Lett.* (in press).
- [16] D. Porras and J. I. Cirac, *Phys. Rev. Lett.* **96**, 250501 (2006).
- [17] J. M. Taylor and T. Calarco, *Phys. Rev. A* **78**, 062331 (2008)
- [18] I. M. Buluta, M. Kitaoka, S. Georgescu, and S. Hasegawa, *Phys. Rev. A* **77**, 062320 (2008).
- [19] T. B. Mitchell, J. J. Bollinger, D. H. E. Dubin, X. -P. Huang, W. M. itano, and R. H. Baughman, *Science* **282**, 1290 (1998)
- [20] W. M. Itano, J. J. Bollinger, J. N. Tan, B. Jelenkovic, X. -P. Huang, and D. J. Wineland, *Science* **279**, 686 (1998)
- [21] M. Drewsen, C. Brodersen, L. Hornekaer, J. S. Hangst, and J. P. Schiffer, *Phys. Rev. Lett.* **81**, 2878 (1998).
- [22] D. H. E. Dubin, *Phys. Rev. Lett.* **71**, 2753 (1993).
- [23] R. Raussendorf and J. Harrington, *Phys. Rev. Lett.* **98**, 190504 (2007).
- [24] D. F. V. James, *Appl. Phys. B* **66**, 181 (1998).
- [25] J. P. Schiffer, *Phys. Rev. Lett.* **70**, 818, (1993).
- [26] P. J. Lee, K.A. Brickman, L. Deslauriers, P. C. Haljan, L.M.Duan, and C. Monroe, *J. Opt. B: Quantum Semiclass.* **7**, S371 (2005).
- [27] S. L. Zhu and Z. D. Wang, *Phys. Rev. Lett.* **91**, 187902 (2003).
- [28] For a review of geometric quantum computation, see E. Sjöqvist, *Physics* **1**, 35 (2008).